

Short-ranged and short-lived charge-density-wave order and pseudogap features in underdoped cuprates superconductors

Andrés Greco and Matías Bejas

Facultad de Ciencias Exactas, Ingeniería y Agrimensura and Instituto de Física Rosario (UNR-CONICET). Av. Pellegrini 250-2000 Rosario-Argentina.

(Dated: June 17, 2011)

The pseudogap phase of high- T_c cuprates is controversially attributed to preformed pairs or to a phase which coexists and competes with superconductivity. One of the challenges is to develop theoretical and experimental studies in order to distinguish between both proposals. Very recently, researchers at Stanford have reported [M. Hashimoto *et al.*, Nat. Phys. **6**, 414 (2010); R.-H. He *et al.*, Science **331**, 1579 (2011)] angle-resolved photoemission spectroscopy experiments on Pb-Bi2201 supporting the point of view that the pseudogap is distinct from superconductivity and associated to a spacial symmetry breaking without long-range order. In this paper we show that many features reported by these experiments can be described in the framework of the t - J model considering self-energy effects in the proximity to a d charge-density-wave instability.

PACS numbers: 74.72.-h, 74.25.Jb, 71.10.Fd, 79.60.-i

Although the solid state physics community agrees on the existence of the pseudogap (PG) phase in underdoped high- T_c superconductors, the origin of the PG and its relation with superconductivity (SC) is not clear from experimental and theoretical studies. Interpretations run from descriptions where the PG is intimately related to SC to others where the PG is distinct from SC and both phases compete.¹ Thus, experimental and theoretical studies are of central interest for solving this puzzle.

Angle-resolved photoemission spectroscopy (ARPES) is a valuable tool for studying the PG phase.² In the pseudogap phase ARPES experiments show, in the normal state below a characteristic temperature T^* , Fermi arcs³⁻⁶ (FAs) (centered along the zone diagonal) instead of the expected Fermi surface (FS). Despite the general consensus about the existence of FAs, their main characteristics are controversial. Some experiments^{3,4} report that near the antinode exists a single gap which is nearly independent of temperature. Moreover, in the superconducting state the gap follows the expected d -wave behavior along the FS. In contrast, other experiments^{5,6} show that the gap follows the d -wave behavior near the node but deviates upward approaching the antinode. In our opinion the difference in the spectra reported by different groups can not only be attributed to the different systems under study. For instance, similar samples at similar doping (see Refs.[4] and [5]) also show the mentioned discrepancy. Although the reason for these differences is not clear, results of Refs.[3] and [4] suggest that FAs are tied to the preformed pair scenario, while results from Refs.[5] and [6] claim that arcs are associated to an order which is distinct from SC.

Recently, ARPES results on Pb-Bi2201 were reported (Refs.[7] and [8]) showing that the PG phase is distinct from SC and associated to a spacial symmetry breaking without long-range order. Since these experiments challenge scenarios about the origin of the PG and FAs, their theoretical support is of high and broad interest.

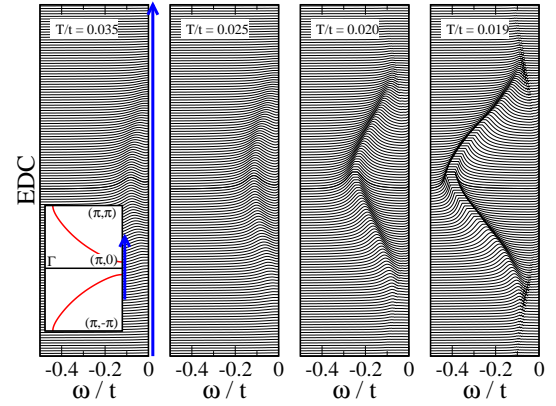


FIG. 1. (Color online) Energy distribution curves in the normal state from a high temperature (left panel) to a lower temperature (right panel) near the d -CDW instability along the antinodal cut shown by an arrow in the inset of the left panel.

In the framework of the t - J model at mean-field level the carriers show a band dispersion $\epsilon_k = -2t_{eff}[\cos(k_x) + \cos(k_y)] - 4t'_{eff} \cos(k_x) \cos(k_y) - \mu$, with $t_{eff} = (t_{\frac{\delta}{2}} + rJ)$ and $t'_{eff} = t'_{\frac{\delta}{2}}$. t , t' and J are the hopping between nearest-neighbor, next-nearest-neighbor and the nearest-neighbor Heisenberg coupling, respectively. δ is the doping away from half-filling, μ is the chemical potential, and rJ is the J -driven hopping term. This mean-field homogeneous Fermi liquid (HFL) phase presents an instability to a d charge-density-wave (d -CDW) state⁹ or a flux phase¹⁰ (FP) below a characteristic temperature T_{FP} which decreases with increasing doping (see Ref.[11] and references therein).

Beyond mean-field level, in the HFL phase and in the proximity to the d -CDW instability, the self-energy

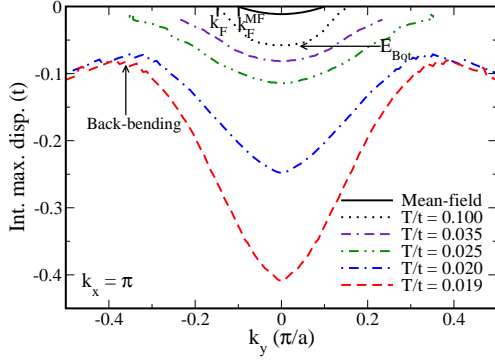


FIG. 2. (Color online) Intensity maximum dispersion, for several temperatures in the normal state, taken along the antinodal cut. Solid line is the predicted mean-field dispersion. At mean-field level the effective parameters are $t_{eff}/t \sim 0.08$ and $t'_{eff}/t \sim -0.017$, while the effective parameters that reproduce the effective band at high temperature (dotted line) are $t_{eff}/t \sim 0.21$ and $t'_{eff}/t \sim -0.03$. Note that the Fermi wave vector \mathbf{k}_F is different from the mean-field value $\mathbf{k}_F^{MF} \sim (\pi, 0.1\pi)$.

$\Sigma(\mathbf{k}, \omega)$ reads¹¹

$$Im \Sigma(\mathbf{k}, \omega) = -\frac{1}{N_s} \sum_{\mathbf{q}} \gamma^2(\mathbf{q}, \mathbf{k}) Im \chi(\mathbf{q}, \omega - \epsilon_{\mathbf{k}-\mathbf{q}}) \times [n_F(-\epsilon_{\mathbf{k}-\mathbf{q}}) + n_B(\omega - \epsilon_{\mathbf{k}-\mathbf{q}})],$$

where n_B and n_F are the Bose and Fermi factors, respectively, and N_s is the number of sites. $\chi(\mathbf{q}, \omega) = (\frac{g}{2})^2 [(8/J)r^2 - \Pi(\mathbf{q}, \omega)]^{-1}$ is the d -CDW susceptibility that diverges, at $\omega = 0$ and $\mathbf{q} = (\pi, \pi)$, and at T_{FP} . $\Pi(\mathbf{q}, \omega)$ is the electronic polarizability calculated with a form factor $\gamma(\mathbf{q}, \mathbf{k}) = 2r[\sin(k_x - q_x/2) - \sin(k_y - q_y/2)]$. Note that since $\mathbf{q} \sim (\pi, \pi)$ the form factor $\gamma(\mathbf{q}, \mathbf{k})$ transforms into $\sim [\cos(k_x) - \cos(k_y)]$ which indicates the d -wave character of the d -CDW. Using the self-energy $\Sigma(\mathbf{k}, \omega)$, the spectral function is calculated as usual. This scenario leads to a PG and FAs which depend on doping and temperature in close agreement with the experiment, and occur via the coupling between quasiparticles (QPs) and the d -CDW soft mode in the proximity to the instability.¹¹⁻¹³ Here after $t'/t = -0.35$ and $J/t = 0.3$. The hopping t and the lattice constant a of the square lattice are used as energy and length units, respectively.

We show here that many aspects observed in Refs.[7] and [8] can be discussed in the framework of Refs.[11], [12], and [13] showing that a theory where the PG phase is distinct from SC and associated with short-range fluctuations in the proximity to a symmetry breaking instability is consistent with the experiment.

Similar to Fig. 1 g-l of Ref.[7], in Fig. 1 we present energy distribution curves (EDC) for momenta along the antinodal cut indicated in the inset. With no loss of generality, results are given in the HFL phase for doping $\delta = 0.10$ and for several temperatures from $T/t = 0.035$ to $T/t = 0.019$ close but above $T_{FP}/t \sim 0.018$. At high

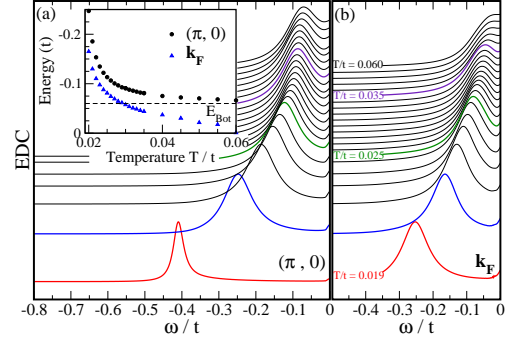


FIG. 3. (Color online) (a) Energy distribution curves for momentum $(\pi, 0)$ for several temperatures. (b) The same as (a) for momentum \mathbf{k}_F . The inset shows the energy position of the maximum of the energy distribution curves as a function of temperature for $\mathbf{k} = (\pi, 0)$ (circles) and \mathbf{k}_F (triangles).

temperature ($T/t = 0.035$), EDC resemble a parabolic-like dispersion as expected for usual metals. Lowering temperature, a PG like feature becomes evident near the antinode and, at the same time, a back-bending occurs in the dispersion. For summarizing the main results of Fig. 1, in Fig. 2, we show (similar to Fig. 1n in Ref.[7]) the intensity maximum dispersion for several temperatures. At high temperature ($T/t \sim 0.1$), no PG is observed near the antinode and a parabola-like dispersion (dotted line), which crosses $\omega = 0$ at $\mathbf{k}_F \sim (\pi, 0.16\pi)$, is obtained. In the figure, we have also plotted results for the mean-field band (solid line). With decreasing temperature a PG opens near the antinode and, as in the experiment, a back-bending (marked by an arrow) is observed beyond \mathbf{k}_F , in addition, the energy of the band bottom (E_{Bot}) at $(\pi, 0)$ moves deeply to lower binding energies. In Ref.[7], the existence of a back-bending beyond \mathbf{k}_F was discussed as a result that rules out preformed pairs and favors a scenario where the PG is distinct from SC. Present results are consistent with that interpretation as discussed below.

Following the comparison with results in Ref.[7], in Figs. 3(a) and 3(b) we have plotted EDC at $(\pi, 0)$ and \mathbf{k}_F , respectively, for several temperatures. For $\mathbf{k} = (\pi, 0)$, the energy of the maximum of the EDC moves, with increasing temperature, toward E_{Bot} as shown by circles in the inset. Figure 3(b) shows that, with increasing temperature, the PG at \mathbf{k}_F closes and, at the same time, fills as in the experiment. In the inset the energy of the maximum of the EDC at \mathbf{k}_F is plotted (triangles) as a function of temperature showing that, for $T/t \gtrsim 0.06$ no PG is observed. Since EDC at \mathbf{k}_F show a maximum at $\omega = 0$ for $T/t \gtrsim 0.06$, we identify the pseudogap temperature with $T^*/t \sim 0.06$. In addition, we also identify the dotted line in Fig. 2 with the effective metallic band (recovered at high temperature) discussed in Ref.[7]. Finally, we note that in the present theory the opening of the PG is not associated to an abrupt transition but to a smooth crossover.

Using the accepted value $t = 0.4$ eV, $T^* \sim 270$ K,

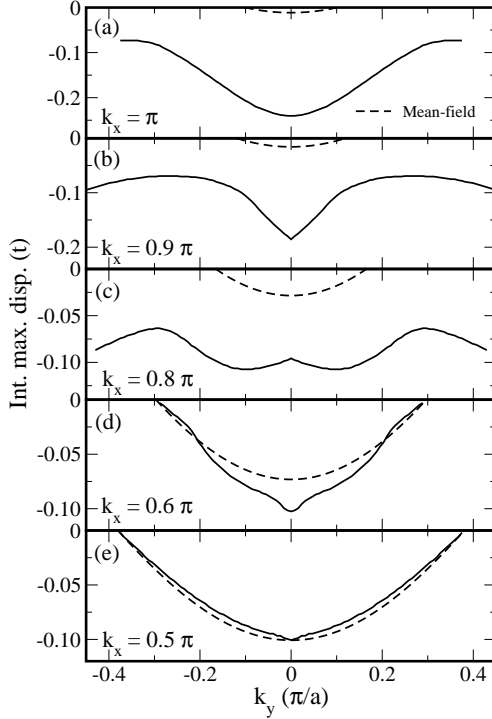


FIG. 4. Intensity maximum dispersion for several cuts, parallel to the antinodal cut, at $T/t = 0.020$. Dashed line in each panel is the predicted mean-field dispersion for the corresponding cut.

$E_{Bot} \sim 25$ meV, and the energy at the back-bending ~ 40 meV. Since our description does not require phenomenological parameters as a value for the PG energy and its temperature dependence, as in other approaches,¹⁴ the agreement with the experiment can be considered satisfactory.

Next, we show predictions of our theory for other cuts on the Brillouin zone. Similar to Fig. 2, in Fig. 4 we have plotted, for $T/t = 0.020$, the intensity maximum dispersions for cuts parallel to the antinodal cut. In each cut, we fix k_x to be $\pi, 0.9\pi, 0.8\pi, 0.6\pi$, and 0.5π , and vary k_y . While for cuts close to the antinode $[(\pi, k_y), (0.9\pi, k_y), \text{ and } (0.8\pi, k_y)]$ a PG and a back-bending are clearly observed, for cuts near the node $[(0.6\pi, k_y) \text{ and } (0.5\pi, k_y)]$ the back-bending and the PG wash out and a FS crossing occurs. This behavior is consistent with the prediction of FAs by present theory.^{11–13} In addition, different to the cuts near the antinode (see Figs. 1 and 3), for cuts near the node the QP peaks (not shown) become sharper and the renormalized dispersion is closer to the bare mean-field band (dashed line). This fact reflects that the effect of the d -CDW mode diminishes approaching the node.¹¹

It is worth to mention that a generic long-range CDW phase may show, qualitatively, some of the features presented here such as, for instance, the back-bending beyond \mathbf{k}_F . Some differences with the long-range CDW point of view are: (a) While in a CDW phase the translational symmetry is broken, in the present theory, the sys-

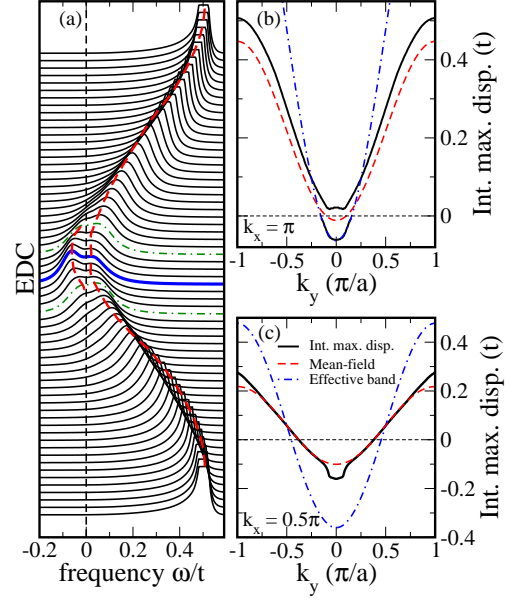


FIG. 5. (Color online) (a) Energy distribution curves along the antinodal cut for $T/t = 0.1$. Thick solid blue line is the energy distribution curve for $\mathbf{k} = (\pi, 0)$. Dashed red lines represent a guide for the eye showing that the double peak structure at both sides of $\omega = 0$ near $\mathbf{k} = (\pi, 0)$ merges into only one peak away from $\mathbf{k} = (\pi, 0)$, which follows the predicted mean-field result. Note that at \mathbf{k}_F (dashed-dotted green line), no pseudogap is observed for this temperature. (b) Intensity maximum dispersion (solid line), the effective band (dashed-dotted line) discussed in text, and the mean-field dispersion (dashed line) along the antinodal cut for $T/t = 0.1$ (c) The same as (b) for the cut $(0.5\pi, k_y)$.

tem is always in the HFL phase but, under the influence of short-range fluctuations. (b) While sharp QP peaks are expected in a CDW phase, our results show broad structures as in the experiment. These broad structures are intrinsic and not related to the instrumental resolution as suggested in Ref.[14]. For explaining the broad spectra observed in the experiment, in Ref.[7] a static density wave order with a finite correlation length was assumed. In addition, it was suggested that the observed fast sink, with decreasing temperature, of the band bottom implies an incommensurate character of the charge order. Both, the broad spectra and the temperature behavior of the band bottom are naturally described by the present picture. We think that this fact suggests, besides of a short correlation length, a slowly dynamical character of the charge order, and these conditions are fulfilled in the fluctuating regime near the instability. Since the discussion about the interpretation of the PG as a phase with long-range order versus a phase without long-range order is highly controversial (see Ref.[15] for a review), we expect that our finding may contribute to the distinction between both scenarios.

Now, we discuss some characteristics of the high temperature phase. In Figs. 5(a) and 5(b), we present EDC and the corresponding intensity maximum dispersions,

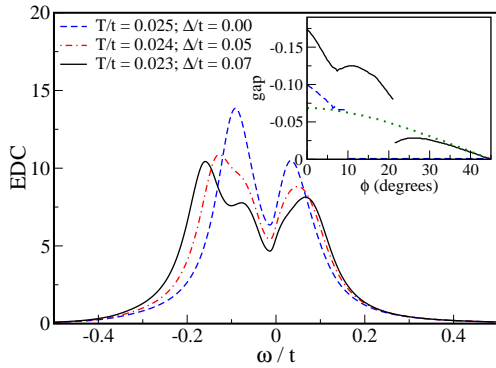


FIG. 6. (Color online) EDC obtained for various superconducting gaps values Δ (see text). Inset: Energy position of the leading gap of the EDC as a function of the FS angle ϕ for the normal state (dashed line) and in the superconducting state (solid line).

respectively, for the antinodal cut at $T/t = 0.1$. Note the broad feature with structure at both sides of $\omega = 0$ at $(\pi, 0)$ [thick solid blue line in Fig. 5(a)]. This double peak structure merges into only one feature away from $(\pi, 0)$ approaching the predicted mean-field band [dashed line in Fig. 5(b)]. The parabola-like band, discussed in Fig. 2 at high temperature, follows the effective band [dashed-dotted line in Fig. 5(b)] for $\omega < 0$. We note that the closing of the PG at $T/t \sim 0.06$ is mainly due to a filling effect which occurs from the merging of the broad peak at $\omega < 0$ with the one at $\omega > 0$. In Fig. 5(c), we have plotted, for the cut $(0.5\pi, k_y)$, the intensity maximum dispersion of the EDC at $T/t = 0.1$. Different to the antinodal cut, the intensity maximum dispersion is closer to the mean-field band (dashed line) for both, $\omega < 0$ and $\omega > 0$. From the experimental point of view, this result means that above T^* , a unique set of parameters might not describe the dispersion for all cuts, as it should be if the high temperature phase can be associated with a usual metal. It is interesting to see whether this prediction may be checked by the experiment.

In Ref.[7], it was reported that with decreasing temperature, the spectra and the leading edge gap near the antinode smoothly become broad and move toward higher binding energy, respectively, with no significant

change below the superconducting critical temperature T_c . At first sight, it would expect that d -CDW fluctuations would be washed out once superconductivity sets in. However, considering that the superconducting gap is smaller than the pseudogap, we can approximate the Green function in the superconducting state as $G_{SC}^{-1}(k, i\omega) = G^{-1}(k, i\omega) + \Delta_k^2 G(k, -i\omega)$, where $G(k, i\omega)$ is the Green function describing the spectral functions of Fig. 3(b), and $\Delta_k = \Delta(\cos k_x - \cos k_y)/2$ is a d -wave superconducting gap. In Fig. 6, we present EDC at \mathbf{k}_F . In the normal state ($\Delta = 0$) (assumed to be the previous result for $T/t = 0.025$), the peaks at both sides of $\omega = 0$ are broad and asymmetric. With increasing Δ (decreasing temperature below T_c), the broad peak slowly moves to lower energies as in the experiment.⁷ It is interesting to note the presence of an inner shoulder which is a direct indication of two distinct energy scales below T_c . A similar shoulder was discussed in Ref.[7], and more clearly reported in Ref.[8] after improving the experimental resolution. We think that an unambiguous experimental confirmation of an inner shoulder (or a peak) below T_c is of fundamental interest for solving the puzzle about one versus two energy scales. The reason for the absence of this shoulder in some ARPES experiments^{3,4} is an open question and out of the scope of the present paper. In the inset of Fig. 6 we plot the energy position of the leading gap of the EDC as a function of the FS angle ϕ from the antinode ($\phi = 0$) to the node ($\phi = 45$ degrees). For $\Delta = 0$ (dashed line), the region near the antinode is gaped leading to Fermi arcs. For $\Delta/t = 0.07$ (solid line), the curve follows the d -wave behavior (dotted line) only near the node, and deviates upward approaching the antinode. It is interesting to see that for Pb-Bi2201, the gap follows this trend in similar way to Refs.[5] and [15] (see Fig. 4S in Ref.[8]).

Concluding, we have shown that the scattering between carriers and d -CDW fluctuations, which occur in the proximity to the d -CDW instability, describes many features observed in recent ARPES experiments. The proposed scenario supports the point of view that the pseudogap is distinct from superconductivity and associated with short-range and short-lived CDW fluctuations.

The authors thank H. Parent, R.-H. He, and R. Zeyher for valuable discussions.

- ¹ S. Hüfner, M.A. Hossain, A. Damascelli, and G.A. Sawatzky, Rep. Prog. Phys. **71**, 062501 (2008). M. R. Norman, D. Pines and C. Kallin, Adv. Phys. **54**, 715 (2005).
- ² A. Damascelli, Z. Hussain, and Z.-X. Shen, Rev. Mod. Phys. **75**, 473 (2003).
- ³ M.R. Norman *et al.*, Nature **392**, 157 (1998). A. Kanigel *et al.*, Nature Physics **2**, 447 (2006). A. Kanigel *et al.*, Phys. Rev. Lett. **99**, 157001 (2007).
- ⁴ M. Shi *et al.*, Phys. Rev. Lett. **101**, 047002 (2008).
- ⁵ K. Terashima *et al.*, Phys. Rev. Lett. **99**, 017003 (2007).
- ⁶ T. Yoshida *et al.*, Phys. Rev. Lett. **103**, 037004 (2009).

- T. Kondo *et al.*, Phys. Rev. Lett. **98**, 267004 (2007). T. Kondo *et al.*, Nature **457**, 296 (2009). K. Tanaka, *et al.*, Science **314**, 1910 (2006). W.S. Lee, *et al.*, Nature **450**, 81 (2007). J.-H. Ma *et al.*, Phys. Rev. Lett. **101**, 207002 (2008).
- ⁷ M. Hashimoto *et al.*, Nature Phys. **6**, 414 (2010).
- ⁸ R.-H. He, *et al.*, Science **331**, 1579 (2011).
- ⁹ S. Chakravarty, R. B. Laughlin, D. K. Morr, and C. Nayak, Phys. Rev. B **63**, 094503 (2001).
- ¹⁰ I. Affleck and J.B. Marston, Phys. Rev. B **37**, 3774 (1988). E. Cappelluti and R. Zeyher, Phys. Rev. B **59**, 6475 (1999).

- ¹¹ A. Greco, Phys. Rev. Lett. **103**, 217001 (2009).
- ¹² A. Greco, Phys. Rev. B **77**, 092503 (2008).
- ¹³ M. Bejas, G. Buzon, A. Greco, and A. Foussats, Phys. Rev. B **83**, 014514 (2011).
- ¹⁴ J. P. F. LeBlanc, J. P. Carbotte, and E. J. Nicol, Phys. Rev. B **83**, 184506 (2011).
- ¹⁵ I. M. Vishik *et al.*, New J. Phys. **12**, 105008 (2010).